

Probabilistic Forecasting with Conditional Generative Networks via Scoring Rule Minimization

Lorenzo Pacchiardi¹ Rilwan A. Adewoyin^{2,3} Peter Dueben⁴ Ritabrata Dutta²

Abstract

Probabilistic forecasting consists of stating a probability distribution for a future outcome based on past observations. In meteorology, ensembles of physics-based numerical models are run to get such distribution. Usually, performance is evaluated with scoring rules, functions of the forecast distribution and the observed outcome. With some scoring rules, calibration and sharpness of the forecast can be assessed at the same time.

In deep learning, generative neural networks parametrize distributions on high-dimensional spaces and easily allow sampling by transforming draws from a latent variable. Conditional generative networks additionally constrain the distribution on an input variable. In this manuscript, we perform probabilistic forecasting with conditional generative networks trained to minimize scoring rule values. In contrast to Generative Adversarial Networks (GANs), no discriminator is required and training is stable. We perform experiments on two chaotic models and a global dataset of weather observations; results are satisfactory and better calibrated than what achieved by GANs.

1. Introduction

In many disciplines (for instance economics and meteorology), practitioners want to forecast future outcomes based on observations up to the present moment. As opposed to a deterministic forecast, a probabilistic one yields uncertainty in the prediction. Probabilistic forecasting (Gneiting & Katzfuss, 2014) is commonplace in Numerical Weather

Prediction (NWP, Palmer, 2012), where physics-based models are run multiple times to obtain an ensemble of forecasts representing the possible evolution of the weather. To assess the performance of NWP systems, Scoring Rules (SRs, Gneiting & Raftery, 2007) are commonly used. SRs are functions quantifying the quality of a probabilistic forecast with respect to the observed outcome. Of all SRs, so-called *strictly proper* ones are minimized in expectation only when the forecast distribution coincides with the data generating one.

Parallely, in the deep learning literature, generative neural networks have been developed to sample from probability distributions on structured and high dimensional spaces. Specifically, the neural network defines a map from a latent variable space to the outcome space, and samples on the latter are obtained by transforming latent variable draws. The distribution is thus implicitly defined, as the density is inaccessible. In *conditional* generative networks, the network output additionally depends on a conditioning variable; by keeping that fixed, samples from a conditional distribution can be obtained.

Generative networks are usually trained in the framework of Generative Adversarial Networks (GANs, Goodfellow et al., 2014; Mirza & Osindero, 2014). There, a *discriminator* network is tasked with distinguishing between generated and true data, and trained against the generator in a min-max setting: the discriminator aims to maximize its discriminative power, while the generative network is trained to minimize it; at convergence, the generative network produces samples from the data generating process. However, the adversarial formulation makes the training of GANs unstable: tuning experience is required to obtain good performances.

Here, we propose to train conditional generative networks using SRs as an objective, for the task of probabilistic forecast. Specifically, we assume to have a long time-series recording of the phenomenon we want to forecast and use this to build a training dataset composed of past observations and targets. Each observation window is used to forecast the corresponding target, and the performance with respect to the realization is assessed using a Scoring Rule, whose value the network is trained to minimize. Compared to GANs, no discriminator or adversarial formulation is needed, which

¹Department of Statistics, University of Oxford, Oxford, UK

²Department of Statistics, University of Warwick, Coventry, UK

³Department of Computer Science and Engineering, Southern University of Science and Technology, Shenzhen, China ⁴Earth System Modelling Section, The European Centre for Medium-Range Weather Forecasts, Reading, UK. Correspondence to: Lorenzo Pacchiardi <lorenzo.pacchiardi@stats.ox.ac.uk>.

makes training and hyperparameters selection easier.

We apply this method to two benchmark models of chaotic systems; with respect to GANs, we find the forecast of our method to better match the realizations: importantly, the calibration of the forecast is drastically improved. We then apply our method to a real-life global dataset of weather observations, with promising results.

The rest of the manuscript is organized as follows. In Section 2, we give some background information on probabilistic forecasting and conditional generative models. Next, in Section 3, we review Scoring Rules and introduce those we will use in our method. In Section 4, we formalize the training objective and algorithm to perform probabilistic forecasting with SRs. Subsequently, we discuss some related works in Section 5 and show some simulation results in Section 6. We conclude in Section 7 mentioning future improvements and open questions.

1.1. Notation

We use upper case X, Y and Z to denote random variables, and their lower-case counterpart to denote observed values. Bold symbols denote vectors, and subscripts to bold symbols denote sample index (for instance, \mathbf{y}_t). Instead, subscripts to normal symbols denote component index (for instance, y_i is the i -th component of \mathbf{y} , and $y_{t,j}$ is the i -th component of \mathbf{y}_t). Finally, we use notation $\mathbf{y}_{j:k} = (\mathbf{y}_j, \mathbf{y}_{j+1}, \dots, \mathbf{y}_{k-1}, \mathbf{y}_k)$, for $j < k$.

2. Background

2.1. Probabilistic forecasting

Consider a temporal stochastic process $(\mathbf{Y}_1, \mathbf{Y}_2, \dots, \mathbf{Y}_n, \dots) \sim P^*$, where $\mathbf{Y}_t \in \mathcal{Y} \subseteq \mathbb{R}^d$; in general, \mathbf{Y}_t 's are not independent. Say we have observed the process up to the n -th time step and obtained a realization $\mathbf{y}_{1:n}$; we want now to obtain a probabilistic forecast for \mathbf{Y}_{n+l} for a given lead time l . In practice, one usually considers a set of conditional models $P_\phi^l(\cdot | \mathbf{y}_{1:n})$ parametrized by parameters $\phi \in \Phi$, and attempts to pick the value of ϕ which provides the best forecast according to some metric. We assume in the following that the model P_ϕ^l only depends on the most recent k observations (the *observation window*); therefore, we denote the probabilistic forecast for \mathbf{Y}_{n+l} by $P_\phi^l(\cdot | \mathbf{y}_{n-k+1:n})$.

2.2. Conditional generative models

A *conditional generative model* defines a conditional distribution by pushing forward a base measure Q over a latent variable $Z \in \mathcal{Z}$ via a map dependent on a set of conditioning variables. Specifically, let us consider a map:

$$T_\phi : \mathcal{Z} \times \mathcal{X} \rightarrow \mathcal{Y},$$

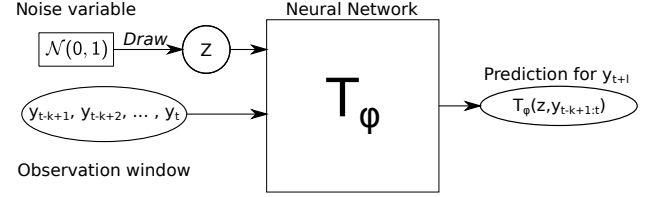


Figure 1. An example of conditional generative network for probabilistic forecast, with a univariate standard normal latent variable.

where \mathcal{X} is the space of conditioning variables. For a given $x \in \mathcal{X}$, the conditional distribution is therefore defined as:

$$P(\cdot | \mathbf{x}) = T_\phi(\cdot; \mathbf{x}) \# Q;$$

the above notation means that, for any set A belonging to the Borel sigma-algebra $\sigma(\mathcal{Y})$:

$$P(A | \mathbf{x}) = Q(\{z \in \mathcal{Z} : T_\phi(z; \mathbf{x}) \in A\}),$$

In practice, samples from $P(\cdot | \mathbf{x})$ are obtained by generating $z \sim Q$ and computing $T(z; \mathbf{x})$.

In the following, we will use a conditional generative model to represent the forecast distribution P_ϕ^l defined above; there, $\mathcal{X} = \mathcal{Y}^k$, so that¹:

$$P_\phi^l(\cdot | \mathbf{y}_{t-k+1:t}) = T_\phi(\cdot; \mathbf{y}_{t-k+1:t}) \# Q.$$

Additionally, we will use Neural Networks (NNs) to represent the map T_ϕ , with ϕ thus representing NN weights. A representation of a conditional generative network for probabilistic prediction is given in Figure 1.

2.3. Adversarial training for conditional generative networks

Conditional generative networks are usually trained in the conditional Generative Adversarial Networks (GANs, [Mirza & Osindero, 2014](#)) framework; here, the generative network T_ϕ attempts to fool a *discriminator* network D_ψ , whose task is distinguishing between generated and true samples. The conditioning variable is fed through both generator and discriminator. More specifically, for the task of learning a distribution $P^*(\cdot | \mathbf{x})$ on \mathbf{Y} conditioned on the realized value \mathbf{x} of another variable $\mathbf{X} \sim \Pi^*$, the training objective is:

$$\min_{\phi} \max_{\psi} \mathbb{E}_{\mathbf{X} \sim \Pi^*} [\mathbb{E}_{\mathbf{Y} \sim P^*(\cdot | \mathbf{x})} [\log D_\psi(\mathbf{Y}; \mathbf{X})] + \mathbb{E}_{\mathbf{Z} \sim Q} [\log(1 - D_\psi(T_\phi(\mathbf{Z}; \mathbf{X}); \mathbf{X}))]],$$

where again Q is a latent variable distribution. In practice, training is performed by iteratively updating ϕ and ψ ([Goodfellow et al., 2014](#)) via Stochastic Gradient Descent (SGD,

¹We omit the lag index l in the notation for the map T_ϕ for simplicity; however, different maps are required to forecast at different lags.

Ruder, 2016). At each step of the training process, the expectation over $\mathbf{X} \sim \Pi^*$ and $\mathbf{Y} \sim P^*(\cdot|\mathbf{Y})$ is estimated using observed data, say $(\mathbf{x}_i, \mathbf{y}_i)$, for some values of i in $1, \dots, N$; usually, a single draw from the latent variable distribution Q for each training sample is used (albeit multiple are possible).

Although the above formulation requires independent data, conditional GANs have been used for time-series forecasting (see for instance, in the meteorology domain, Bihlo, 2021; Ravuri et al., 2021). In Algorithm 1, we show a single epoch (i.e., a loop on the full training dataset) of conditional GAN training with for the considered probabilistic forecast setting; for simplicity, we consider batch size equal to one, but using larger batches is indeed possible².

Algorithm 1 Single epoch conditional GAN training.

Require: Parametric map T_ϕ , discriminator network D_ψ , learning rates ϵ, γ .

- 1: **for** t from k up to $n - l$ **do**
- 2: Sample a **single** \mathbf{z}
- 3: Obtain $\hat{\mathbf{y}}_{t+l}^{(\phi)} = T_\phi(\mathbf{z}, \mathbf{y}_{t-k+1:t})$
- 4: Update

$$\psi \leftarrow \psi + \gamma \cdot \nabla_\psi \left[\log D_\psi(\mathbf{y}_{t+l}, \mathbf{y}_{t-k+1:t}) + \log(1 - D_\psi(\hat{\mathbf{y}}_{t+l}^{(\phi)}, \mathbf{y}_{t-k+1:t})) \right]$$

- 5: Update $\phi \leftarrow \phi - \epsilon \cdot \nabla_\phi \log(1 - D_\psi(\hat{\mathbf{y}}_{t+l}^{(\phi)}, \mathbf{y}_{t-k+1:t}))$
 - 6: **end for**
-

3. Scoring Rules

A Scoring Rule (SR) S (Dawid & Musio, 2014; Gneiting & Raftery, 2007) is a function of a probability distribution and of an observation. For a forecast distribution P over \mathcal{Y} and an observation $\mathbf{y} \in \mathcal{Y}$, $S(P, \mathbf{y})$ represents the *penalty* assigned to P when \mathbf{y} occurs.³

If \mathbf{y} is the realization of a random variable $\mathbf{Y} \sim Q$, the expected SR can be defined as:

$$S(P, Q) := \mathbb{E}_{\mathbf{Y} \sim Q} S(P, \mathbf{Y}).$$

A SR S is said to be *proper* relative to a set of distributions $\mathcal{P}(\mathcal{Y})$ over \mathcal{Y} if

$$S(Q, Q) \leq S(P, Q) \quad \forall P, Q \in \mathcal{P}(\mathcal{Y}),$$

²Algorithm 1 updates the discriminator once every generator update; however, multiple discriminator updates can be done. Indeed, the theoretical guarantees for GAN training (Goodfellow et al., 2014) consider the discriminator to be trained until convergence for each generator update.

³Some authors (Gneiting & Raftery, 2007) consider $S(P, \mathbf{y})$ to represent a *reward* rather than a penalty, which is equivalent up to change of sign.

i.e., if the expected Scoring Rule is minimized in \mathcal{P} when $P = Q$. Moreover, S is *strictly proper* relative to $\mathcal{P}(\mathcal{Y})$ if $P = Q$ is the unique minimum. If a forecaster is evaluated by a strictly proper Scoring Rule, they will be encouraged to state their true belief (Gneiting & Raftery, 2007).

3.1. Some scoring rules

We now introduce some common SRs; let $\mathbf{X}, \mathbf{X}' \sim P$ be independent samples for the forecast distribution P .

Energy Score The energy score is given by⁴:

$$S_E^{(\beta)}(P, \mathbf{y}) = 2 \cdot \mathbb{E} \|\mathbf{X} - \mathbf{y}\|_2^\beta - \mathbb{E} \|\mathbf{X} - \mathbf{X}'\|_2^\beta, \quad (1)$$

where $\beta \in (0, 2)$. This is a strictly proper Scoring Rule for the class of probability measures P such that $\mathbb{E}_{\mathbf{X} \sim P} \|\mathbf{X}\|_2^\beta < \infty$ (Gneiting & Raftery, 2007). The Energy Score is related to the Energy distance, which is a metric between probability distributions (Rizzo & Székely, 2016). We will fix $\beta = 1$ in the rest of this work.

Kernel Score For a positive definite kernel $k(\cdot, \cdot)$, the kernel Scoring Rule can be defined as (Gneiting & Raftery, 2007):

$$S_k(P, \mathbf{y}) = \mathbb{E}[k(\mathbf{X}, \mathbf{X}')] - 2 \cdot \mathbb{E}[k(\mathbf{X}, \mathbf{y})].$$

The Kernel Score is connected to the squared Maximum Mean Discrepancy (MMD, Gretton et al., 2012) relative to the kernel k . S_k is proper for the class of probability distributions for which $\mathbb{E}[k(\mathbf{X}, \mathbf{X}')] is finite (by Theorem 4 in Gneiting & Raftery, 2007). Additionally, it is strictly proper under conditions on k ensuring that the MMD is a metric for probability distributions on \mathcal{Y} (Gretton et al., 2012). These conditions are satisfied, among others, by the Gaussian kernel (which we will use in this work):$

$$k(\mathbf{x}, \mathbf{y}) = \exp \left(-\frac{\|\mathbf{x} - \mathbf{y}\|_2^2}{2\gamma^2} \right), \quad (2)$$

in which γ is a scalar bandwidth.

Variogram Score The Variogram Score (Scheuerer & Hamill, 2015) aims to capture the correlation between different components of the data. Specifically, it is defined as:

$$S_V^{(p)}(P, \mathbf{y}) = \sum_{i,j=1}^d w_{ij} (|y_i - y_j|^p - \mathbb{E}|X_i - X_j|^p)^2,$$

⁴The probabilistic forecasting literature (Gneiting & Raftery, 2007) use a different convention of the energy score and the subsequent kernel score, which amounts to multiplying our definitions by 1/2. We follow here the convention used in the statistical inference literature (Rizzo & Székely, 2016; Chérif-Abdellatif & Alquier, 2020; Nguyen et al., 2020; Pacchiardi & Dutta, 2020)

where $p > 0$, the sum is over all pairs of components and $w_{ij} > 0$ are fixed weights. In [Scheuerer & Hamill, 2015](#), the variogram score is used to assess performance for a spatial dataset, by setting w_{ij} to be inversely proportional to the spatial distance; in this way, the authors argue, the dependence structure in the data is captured.

However, the variogram score is proper but not strictly so; in fact, it is invariant to change of sign and shift by a constant of all components of \mathbf{X} . Additionally, it only depends on the moments of P up to order $2p$ ([Scheuerer & Hamill, 2015](#)). We will fix $p = 1$ in the rest of this work.

Sum of scoring rules Assume now the observation space \mathcal{Y} is structured, as is the case for spatial data on a grid. As mentioned above, the Variogram Score allows to input information on the spatial dependence structure, but it is not strictly proper. On the other hand, the Kernel and Energy Scores are strictly proper but discard the spatial structure.

We can however obtain a strictly proper SR by adding, for instance, the Energy and the Variogram scores, as stated by the following Lemma (proof in Appendix A).

Lemma 1. *Consider now two proper SRs S_1 and S_2 , and let $w_1, w_2 > 0$; the weighted sum:*

$$S_+(P, \mathbf{y}) = w_1 \cdot S_1(P, \mathbf{y}) + w_2 \cdot S_2(P, \mathbf{y})$$

is a proper SR. Additionally, if at least one of S_1 and S_2 are strictly proper, then S_+ is strictly proper as well.

Thus, a Scoring rule defined by the weighted sum of any strictly proper SR and the Variogram Score is strictly proper and able to encode spatial information via the weights w_{ij} .

3.2. Prequential Scoring Rule

Let us go back now to the forecast setting introduced in Section 2.1. Having observed $\mathbf{y}_{1:n}$, we want to exploit the information therein to select ϕ giving the best forecast model P_ϕ^l . We use a sliding window approach: for a given t , we assess the performance of the model $P_\phi^l(\cdot | \mathbf{y}_{t-k+1:t})$ on the realization \mathbf{y}_{t+l} using a strictly proper SR S . Then we cumulate this value over t and look for ϕ minimizing this quantity, namely:

$$\phi_n^* = \arg \min_{\phi} \sum_{t=k}^{n-l} S(P_\phi^l(\cdot | \mathbf{y}_{t-k+1:t}), \mathbf{y}_{t+l}). \quad (3)$$

Following [Dawid, 1984](#), the formulation in Eq. (3.2) is *predictive sequential* (or *prequential*) as we consider inference to have the aim of making sequential probabilistic forecasts for future observations. Therefore, we refer to the objective in Eq. (3.2) as the prequential SR.

4. Training the generative network via scoring rule minimization

Recall that the map T_ϕ is represented by a NN with weights ϕ . We train therefore the NN to minimize the objective in Eq. (3.2), which is equivalent to:

$$J(\phi) = \frac{1}{N} \sum_{t=k}^{n-l} S(T_\phi(\cdot; \mathbf{y}_{t-k+1:t}) \# Q, \mathbf{y}_{t+l}), \quad (4)$$

where $N = n - l - k + 1$.

Let now $\ell_t(\phi) = S(T_\phi(\cdot; \mathbf{y}_{t-k+1:t}) \# Q, \mathbf{y}_{t+l})$. When the training objective is an average over a large number of terms, Stochastic Gradient Descent (SGD, [Ruder, 2016](#)) is commonly used. Specifically, a random subset of indices $\mathcal{T} \subseteq \{k, k+1, \dots, n-l-1, n-l\}$ (a *batch*) is considered; then, the gradient of the loss on the corresponding samples,

$$\frac{1}{|\mathcal{T}|} \nabla_{\phi} \sum_{t \in \mathcal{T}} \ell_t(\phi) = \frac{1}{|\mathcal{T}|} \sum_{t \in \mathcal{T}} \nabla_{\phi} \ell_t(\phi), \quad (5)$$

is computed and used to update ϕ . This procedure is sound as the above is an unbiased estimate of $\nabla_{\phi} J(\phi)$ over the random batch.

In the present setting, in general we cannot evaluate explicitly $\ell_t(\phi)$, as that depends on the full distribution $T_\phi(\cdot; \mathbf{y}_{t-k+1:t}) \# Q$. However, replacing $\nabla_{\phi} \ell_t(\phi)$ in Eq. (4) with an unbiased estimate $\widehat{\nabla_{\phi} \ell_t(\phi)}$ does not hinder the correctness of the method, as the resulting average $\frac{1}{|\mathcal{T}|} \sum_{t \in \mathcal{T}} \widehat{\nabla_{\phi} \ell_t(\phi)}$ is still an unbiased estimate of $\nabla_{\phi} J(\phi)$.

Unbiased gradient estimates $\widehat{\nabla_{\phi} \ell_t(\phi)}$ can be obtained whenever $S(P, \mathbf{y})$ can be written as an expectation over (possibly multiple) samples from P , as is the case for all scoring rules introduced in Section 3. More details and specific expressions of unbiased estimates are given in Appendix B.

In Algorithm 2, we show how to train the generative network for probabilistic forecasting for a single epoch using SGD, with batch size equal to one. In contrast to the conditional GAN approach introduced in Section 2.3, our approach requires multiple samples from the generative network at each iteration; however, in our simulation study (see Section 6) we found a small number of samples (10 for the high-dimensional example) to be enough for stable training. On the other hand, our approach has the substantial advantage of not requiring a discriminator network and adversarial formulation. That makes training and hyperparameter selection easier; additionally, the loss on a validation set can be monitored during training to perform early stopping.

5. Related works

Estimating probabilistic models by minimizing SR values have been suggested before: [Dawid et al., 2016](#) studied the

Algorithm 2 Single epoch Generative-SR training.

Require: Parametric map T_ϕ , SR S , learning rate ϵ .

- 1: **for** t from k up to $n - l$ **do**
 - 2: Sample **multiple** $\mathbf{z}_1, \dots, \mathbf{z}_m$
 - 3: Obtain $\hat{\mathbf{y}}_{t+l}^{(j)} = T_\phi(\mathbf{z}_j, \mathbf{y}_{t-k+1:t})$
 - 4: Obtain unbiased estimate $\hat{S}(P_\phi(\cdot | \mathbf{y}_{t-k+1:t}), \mathbf{y}_{t+l})$
 - 5: Update $\phi \leftarrow \phi - \epsilon \cdot \nabla_\phi \hat{S}(P_\phi(\cdot | \mathbf{y}_{t-k+1:t}), \mathbf{y}_{t+l})$
 - 6: **end for**
-

statistical properties of minimum SR inference for independent and identically distributed data. Dawid & Musio, 2013 inferred parameters for spatial models by minimizing SRs, considering however models for which the conditional distribution in each location given all the others is available. Instead, Dawid & Musio, 2015 considered model selection based on proper SRs, also studying a prequential application for time series data.

In some sense, our technique modifies the conditional GAN framework by replacing the discriminator with a SR. For unconditional generative networks, a similar approach was explored in Li et al., 2015; Dziugaite et al., 2015, where the MMD between a set of generated and observed data was minimized. In the conditional setting, Bouchacourt et al., 2016 used a method corresponding to our formulation with the Energy Score. However, they motivated it using different arguments and considered independent samples in contrast to our forecast formulation. Similar to the latter, Gritsenko et al., 2020 trained a generative network via a generalized Energy Distance for a speech synthesis task, again considering independent samples. Additionally, they aimed to generate a single sample for a fixed value of the conditioning variable, and they resorted to generative models as a tool to better learn in presence of multiple modes. As such, they did not assess the probabilistic performance of the method.

As for our specific application to the global weather forecast dataset, data-driven weather forecasting with deep learning was pioneered in Dueben & Bauer, 2018; see also, among others, Scher, 2018; Scher & Messori, 2019 and Weyn et al., 2019. All above works provided however deterministic forecasts. A smaller number of studies attempted to perform probabilistic forecasting: Scher & Messori, 2021 trained NNs with a deterministic prediction loss and built ensembles of them using different strategies. This approach is however not guaranteed to lead to the correct probability distribution. Bihlo, 2021 used conditional GANs for a similar task; however, they found the GAN forecasts to be underdispersed, so they needed to consider an ensemble of GANs to increase the forecast spread; again, this is not guaranteed to lead to the correct distribution. Finally, Ravuri et al., 2021 exploited GANs for an extremely large precipitation now-

casting task (i.e., predicting for small lead time), obtaining good deterministic and probabilistic performance.

6. Simulation Study

We present here simulation results for data generated from two time-series models (a univariate and a multivariate one), together with a real data example from meteorology. In all cases, we consider a long time series and split it into a training, validation and test set. We train the network on the training set, use the loss on the validation set to perform early stopping and select hyperparameters, and compare performance across different methods on the test set.

For all examples, we train generative conditional models following our proposed approach with the Energy and Kernel Scores. For the multivariate cases, we also consider the sum between Kernel and Variogram (which we term “Kernel-Variogram” in the following) or Energy and Variogram scores (“Energy-Variogram”). For the Kernel Score, we tune γ in the Gaussian kernel from the validation set as discussed in Appendix E.1. For the Variogram score, we consider a weight matrix inversely proportional to the relevant distance for the considered example. In all examples, the components of the latent variable \mathbf{Z} are sampled independently from a standard normal distribution. For the first two examples, we compare our approach with GANs; additionally, we use fully connected NNs for both the generative network and discriminator. In the final example, we use instead a convolutional architecture for the generative network (detailed below).

To achieve better performance, we train our methods with 5 different learning rate values and select the one with the smallest loss on the validation set. For GANs, we try 5 different learning rate values for both discriminator and generator (thus 25 combinations) and select those with better performance according to the Energy Score. Additional experimental details are given in Appendix E.

On the test set, we assess the calibration of the probabilistic forecast by the *calibration error* (the discrepancy between credible intervals in the forecast distribution and the actual frequencies). We also evaluate how close the mean of the forecast distribution is to the observation by the *Normalized Root Mean-Square Error* (NRMSE) and the *coefficient of determination* R^2 ; we detail all these metrics in Appendix C. As all these metrics are for scalar variables, we compute their values independently for each component and average over them.

6.1. Lorenz63 model

The Lorenz63 model (Lorenz, 1963) is a 3-dimensional chaotic system defined by the following differential equa-

Table 1. Performance on test set of the probabilistic forecasts obtained with the different methods, for the Lorenz63 model. Cal. error and NRMSE: the smaller, the better. R^2 : the larger, the better.

	Cal. error	NRMSE	R^2
Energy	0.0370	0.0293	0.9692
Kernel	0.1220	0.0155	0.9913
GAN	0.4930	0.0880	0.7212

Table 2. Performance on test set of the probabilistic forecasts obtained with the different methods, for the Lorenz96 model. Cal. error and NRMSE: the smaller, the better. R^2 : the larger, the better.

	Cal. error	NRMSE	R^2
Energy	0.1091	0.0175	0.9925
Kernel	0.1334	0.0172	0.9929
Energy-Variogram	0.1427	0.0174	0.9927
Kernel-Variogram	0.1291	0.0149	0.9946
GAN	0.4872	0.0873	0.8151

tions:

$$\frac{dx}{dt} = \sigma(y - x),$$

$$\frac{dy}{dt} = x(\rho - z) - y,$$

$$\frac{dz}{dt} = xy - \beta z.$$

We consider $\sigma = 10$, $\rho = 28$, $\beta = 2.667$ and integrate the model using Euler scheme with $dt = 0.01$ starting from $x = 0, y = 1, z = 1.05$. We discard the first 10 time units and integrate the model for additional 9000 time units, during which we record the value of y every $\Delta t = 0.3$ and discard the values of x and z . From this dataset, we take the first 60% of timesteps as training set, the following 20% as validation and the remaining 20% as test. We then train the networks to forecast the values of y with lead $l = 1$ from an observation window of size $k = 10$.

In Table 1, we report calibration error, NMRSE and R^2 on the test set, for all considered methods. According to the last two metrics, the forecast mean obtained with the Kernel Score better represents the observations; calibration is instead better with the Energy Score. In Figure 2, we visualize observation and forecast (median and 99% credible interval) for a portion of the test set, for GAN and Energy Score; for the latter, the median forecast closely matches the observation. Additionally, GAN produces severely under-dispersed forecasts, while the credible sets for the Energy Score contain the observation most of the times. Similar plots for the Kernel Score are presented in Appendix F.1.

6.2. Lorenz96 model

The Lorenz96 model (Lorenz, 1996) is a toy representation of atmospheric behavior containing slow (\mathbf{x}) and fast (\mathbf{y}) evolving variables. Specifically, the evolution of the vari-

ables is determined by the following differential equations⁵:

$$\begin{aligned} \frac{dx_k}{dt} &= -x_{k-1}(x_{k-2} - x_{k+1}) - x_k + 20 - \sum_{j=J(k-1)+1}^{kJ} y_j; \\ \frac{dy_j}{dt} &= -100y_{j+1}(y_{j+2} - y_{j-1}) - 10y_j + X_{\text{int}[(j-1)/J]+1}, \end{aligned}$$

where $k = 1, \dots, K$, and $j = 1, \dots, JK$, and cyclic boundary conditions are assumed, so that index $k = K + 1$ corresponds to $k = 1$ and similarly for j . The above equations connect the fast and slow variables in a cyclic way. Additionally, x_k reciprocally depends on J fast variables.

Following Gagne et al., 2020, we consider $K = 8$, $J = 32$ and integrate the above equations with RK4 scheme with $dt = 0.001$, starting from $x_k = y_j = 0$ for $k = 2, \dots, K$ and $j = 2, \dots, JK$ and $x_1 = y_1 = 1$. We discard the first 2 time units and record the values of \mathbf{x} every $\Delta t = 0.2$ (which corresponding to roughly one atmospheric day with respect to predictability, Gagne et al., 2020). We do this for additional 4000 time units, and split the resulting dataset in training, validation and test according to the proportions 60%, 20% and 20%. We then forecast the values of \mathbf{x} with lead $l = 1$ from an observation window of size $k = 10$.

In Table 2, we report calibration error, NMRSE and R^2 on the test set, for all considered methods. The forecast mean performs fairly similar with all instances of our method, while GAN performs worse. Again, calibration is better with the Energy Score. In Figure 3, we visualize observation and forecast (median and 99% credible interval) for all 8 components of \mathbf{x} ; we do this for a portion of the test set and for GAN and Energy Score; for the latter, the median forecast closely matches the observation; the performance is slightly worse for GAN. In both cases, the 99% credible intervals are invisible at the represented scale. Similar plots for the Kernel, Energy-Variogram and Kernel-Variogram Scores are presented in Appendix F.2.

⁵The equations presented here are a specific case for simplicity; check Appendix D for the full model.

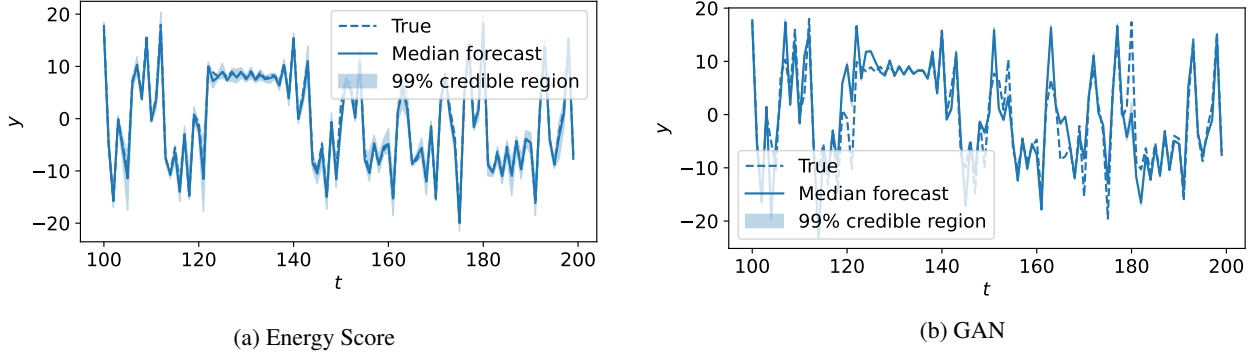


Figure 2. Results with the Energy Score and GAN for the Lorenz63 model. Panels show observations, median forecast and 99% credible interval for a portion of the test set.

6.3. WeatherBench dataset

As a real data example, we consider the WeatherBench dataset (Rasp et al., 2020), which is a benchmark dataset for data-driven weather forecasting. Specifically, Weatherbench contains the hourly value of several atmospheric fields from the year 1979 to 2018, obtained from the reanalysis ERA5 (Hersbach et al., 2020). Field values are available on a grid at different resolutions; we consider here the coarser one (5.625° over both longitude and latitude), corresponding to a 32×64 grid. Additionally, we consider a single observation per day (12:00 UTC) and the 500 hPa geopotential (Z500) variable, which we use both as observation and target. We forecast with a lead of 3 days ($l = 3$) from a single observation ($k = 1$). We use the years from 1979 to 2006 as training set, 2007 to 2016 as validation test and 2017 to 2018 as test set.

We use a U-NET architecture (Olaf et al., 2015), which is an encoder-decoder structure, where each subsequent layer of the encoder outputs a downsampled latent representation of the input variables. The final output of the encoder is passed to a bottleneck layer, which performs no up/down scaling. The output of this bottleneck layer is then passed to the decoder. Conversely to the encoder, each subsequent layer of the decoder outputs an upsampled latent representation of the bottleneck layer output. Additionally, skip connections allow information to pass directly between layers of the encoder and decoder at the same scale; in this way, both large scale structures and high-frequency information contributes to the output. The latent variable \mathbf{Z} is summed to the latent representation in the bottleneck layer.

For this example, we were unable to use the Energy-Variogram Score due to GPU memory limitation. In Table 3, we report calibration error, NMRSE and R^2 on the test set, for all remaining methods. The mean prediction with the Kernel-Variogram Score is slightly better than the other methods; again, the calibration is better with the Energy

Table 3. Performance on test set of the probabilistic forecasts obtained with the different methods, for the WeatherBench dataset. Cal. error and NRMSE: the smaller, the better. R^2 : the larger, the better.

	Cal. error	NRMSE	R^2
Energy	0.0723	0.1252	0.4667
Kernel	0.0992	0.1256	0.4627
Kernel-Variogram	0.0907	0.1237	0.4828

Score. In Figure 4 we show the realization and 5 different predictions obtained with the Kernel-Variogram Score, for a specific date in the test set. The predictions are close to the verification but differ slightly. Figures for the same date and for the other methods are shown in Appendix F.3.1; additionally, in Appendix F.3.2, we show similar plots to what presented for the lower-dimensional examples for a selection of locations on the grid.

7. Conclusions

We have introduced an intuitively appealing framework to perform probabilistic forecasting based on conditional generative models trained via Scoring Rule minimization.

In our simulations study, our method provided better results than GANs, especially in terms of calibration. Likely, the GAN performance could be improved by more careful hyperparameter selection; however, the fact that superior performances were obtained by our method with less hand-tuning is a key advantage.

In follow-up versions of this work, we plan to:

- develop SRs capturing the structure for spatial data;
- perform more detailed simulations for the WeatherBench dataset, considering different lead times, ob-

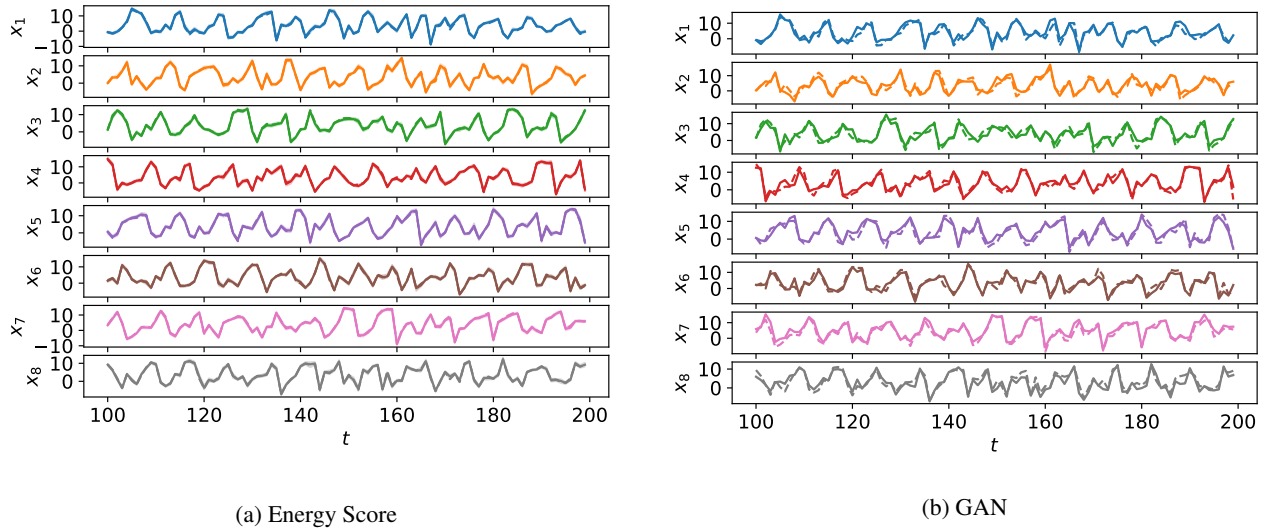


Figure 3. Results with the Energy Score and GAN for the Lorenz96 model. Panels show observations (dashed line), median forecast (solid line) and 99% credible interval (shaded region) for a portion of the test set. That is done for all 8 components of \mathbf{x} . In both cases, credible intervals are invisible at the represented scale.

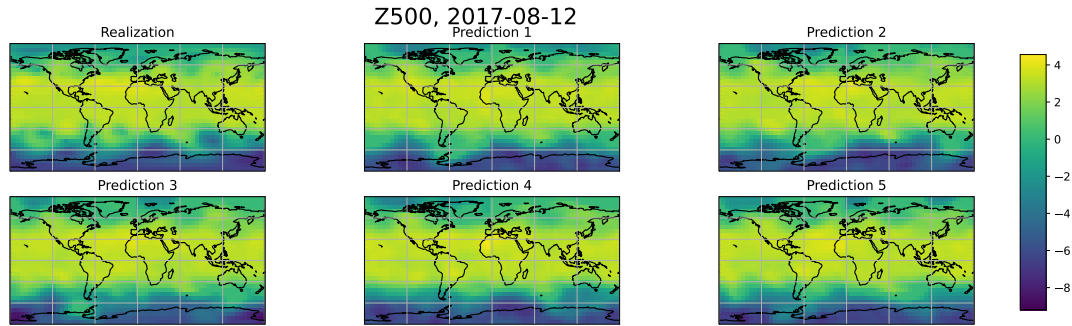


Figure 4. Realization and example of predictions obtained with the Kernel-Variogram Score for a specific date in the test set for the WeatherBench dataset. The predictions capture the main features but are slightly different from each other.

served fields and resolution;

- investigate the theoretical properties of the minimizer of the prequential score, following the strategy suggested in Dawid & Musio, 2015.

Software and Data

Python code for reproducing the experiments will be available at: [text](#).

Acknowledgements

LP is supported by the EPSRC and MRC through the OxWaSP CDT programme (EP/L016710/1), which also funds the computational resources used to perform this

work. RD is funded by EPSRC (grant nos. EP/V025899/1, EP/T017112/1) and NERC (grant no. NE/T00973X/1). We thank Geoff Nicholls, Christian Robert and Peter Watson for valuable feedback and suggestions.

References

- Bihlo, A. A generative adversarial network approach to (ensemble) weather prediction. *Neural Networks*, 139: 1–16, 2021.
- Bouchacourt, D., Mudigonda, P. K., and Nowozin, S. DISCO nets: DISsimilarity COefficient networks. *Advances in Neural Information Processing Systems*, 29: 352–360, 2016.

- Chérif-Abdellatif, B.-E. and Alquier, P. MMD-Bayes: Robust Bayesian estimation via maximum mean discrepancy. In *Symposium on Advances in Approximate Bayesian Inference*, pp. 1–21. PMLR, 2020.
- Dawid, A. P. Present position and potential developments: Some personal views statistical theory the prequential approach. *Journal of the Royal Statistical Society: Series A (General)*, 147(2):278–290, 1984.
- Dawid, A. P. and Musio, M. Estimation of spatial processes using local scoring rules. *AStA Advances in Statistical Analysis*, 97(2):173–179, 2013.
- Dawid, A. P. and Musio, M. Theory and applications of proper scoring rules. *Metron*, 72(2):169–183, 2014.
- Dawid, A. P. and Musio, M. Bayesian model selection based on proper scoring rules. *Bayesian analysis*, 10(2):479–499, 2015.
- Dawid, A. P., Musio, M., and Ventura, L. Minimum scoring rule inference. *Scandinavian Journal of Statistics*, 43(1):123–138, 2016.
- Dueben, P. D. and Bauer, P. Challenges and design choices for global weather and climate models based on machine learning. *Geoscientific Model Development*, 11(10):3999–4009, 2018.
- Dziugaite, G. K., Roy, D. M., and Ghahramani, Z. Training generative neural networks via maximum mean discrepancy optimization. *arXiv preprint arXiv:1505.03906*, 2015.
- Gagne, D. J., Christensen, H. M., Subramanian, A. C., and Monahan, A. H. Machine learning for stochastic parameterization: Generative adversarial networks in the Lorenz’96 model. *Journal of Advances in Modeling Earth Systems*, 12(3):e2019MS001896, 2020.
- Gneiting, T. and Katzfuss, M. Probabilistic forecasting. *Annual Review of Statistics and Its Application*, 1:125–151, 2014.
- Gneiting, T. and Raftery, A. E. Strictly proper scoring rules, prediction, and estimation. *Journal of the American statistical Association*, 102(477):359–378, 2007.
- Goodfellow, I., Pouget-Abadie, J., Mirza, M., Xu, B., Warde-Farley, D., Ozair, S., Courville, A., and Bengio, Y. Generative adversarial nets. *Advances in neural information processing systems*, 27, 2014.
- Gretton, A., Borgwardt, K. M., Rasch, M. J., Schölkopf, B., and Smola, A. A kernel two-sample test. *The Journal of Machine Learning Research*, 13(1):723–773, 2012.
- Gritsenko, A. A., Salimans, T., Berg, R. v. d., Snoek, J., and Kalchbrenner, N. A spectral energy distance for parallel speech synthesis. *arXiv preprint arXiv:2008.01160*, 2020.
- Hersbach, H., Bell, B., Berrisford, P., Hirahara, S., Horányi, A., Muñoz-Sabater, J., Nicolas, J., Peubey, C., Radu, R., Schepers, D., et al. The ERA5 global reanalysis. *Quarterly Journal of the Royal Meteorological Society*, 146(730):1999–2049, 2020.
- Li, Y., Swersky, K., and Zemel, R. Generative moment matching networks. In *International Conference on Machine Learning*, pp. 1718–1727. PMLR, 2015.
- Lorenz, E. N. Deterministic nonperiodic flow. *Journal of atmospheric sciences*, 20(2):130–141, 1963.
- Lorenz, E. N. Predictability: A problem partly solved. In *Proc. Seminar on predictability*, volume 1, 1996.
- Mirza, M. and Osindero, S. Conditional generative adversarial nets. *arXiv preprint arXiv:1411.1784*, 2014.
- Nguyen, H. D., Arbel, J., Lü, H., and Forbes, F. Approximate Bayesian computation via the energy statistic. *IEEE Access*, 8:131683–131698, 2020.
- Olaf, R., Philipp, F., and Thomas, B. U-Net: Convolutional networks for biomedical image segmentation, 2015.
- Pacchiardi, L. and Dutta, R. Score matched conditional exponential families for likelihood-free inference. *arXiv preprint arXiv:2012.10903*, 2020.
- Pacchiardi, L. and Dutta, R. Generalized Bayesian likelihood-free inference using scoring rules estimators. *arXiv preprint arXiv:2104.03889*, 2021.
- Palmer, T. Towards the probabilistic Earth-system simulator: a vision for the future of climate and weather prediction. *Quarterly Journal of the Royal Meteorological Society*, 138(665):841–861, 2012.
- Park, M., Jitkrittum, W., and Sejdinovic, D. K2-ABC: Approximate Bayesian computation with kernel embeddings. In *Artificial Intelligence and Statistics*, 2016.
- Paszke, A., Gross, S., Massa, F., Lerer, A., Bradbury, J., Chanan, G., Killeen, T., Lin, Z., Gimelshein, N., Antiga, L., Desmaison, A., Kopf, A., Yang, E., DeVito, Z., Raison, M., Tejani, A., Chilamkurthy, S., Steiner, B., Fang, L., Bai, J., and Chintala, S. PyTorch: An imperative style, high-performance deep learning library. In Wallach, H., Larochelle, H., Beygelzimer, A., d’Alché-Buc, F., Fox, E., and Garnett, R. (eds.), *Advances in Neural Information Processing Systems 32*, pp. 8024–8035. Curran Associates, Inc., 2019.

- Radev, S. T., Mertens, U. K., Voss, A., Ardizzone, L., and Köthe, U. BayesFlow: Learning complex stochastic models with invertible neural networks. *arXiv preprint arXiv:2003.06281*, 2020.
- Rasp, S., Dueben, P. D., Scher, S., Weyn, J. A., Mouatadid, S., and Thuerey, N. WeatherBench: a benchmark data set for data-driven weather forecasting. *Journal of Advances in Modeling Earth Systems*, 12(11):e2020MS002203, 2020.
- Ravuri, S., Lenc, K., Willson, M., Kangin, D., Lam, R., Mirowski, P., Fitzsimons, M., Athanassiadou, M., Kashem, S., Madge, S., et al. Skillful precipitation now-casting using deep generative models of radar. *arXiv preprint arXiv:2104.00954*, 2021.
- Rizzo, M. L. and Székely, G. J. Energy distance. *Wiley interdisciplinary reviews: Computational statistics*, 8(1): 27–38, 2016.
- Ruder, S. An overview of gradient descent optimization algorithms. *arXiv preprint arXiv:1609.04747*, 2016.
- Scher, S. Toward data-driven weather and climate forecasting: Approximating a simple general circulation model with deep learning. *Geophysical Research Letters*, 45(22):12–616, 2018.
- Scher, S. and Messori, G. Weather and climate forecasting with neural networks: using general circulation models (GCMs) with different complexity as a study ground. *Geoscientific Model Development*, 12(7):2797–2809, 2019.
- Scher, S. and Messori, G. Ensemble methods for neural network-based weather forecasts. *Journal of Advances in Modeling Earth Systems*, 13(2), 2021.
- Scheuerer, M. and Hamill, T. M. Variogram-based proper scoring rules for probabilistic forecasts of multivariate quantities. *Monthly Weather Review*, 143(4):1321–1334, 2015.
- Weyn, J. A., Durran, D. R., and Caruana, R. Can machines learn to predict weather? Using deep learning to predict gridded 500-hPa geopotential height from historical weather data. *Journal of Advances in Modeling Earth Systems*, 11(8):2680–2693, 2019.

Appendix

A. Proof of Lemma 1

Proof. By the definition of proper SR, we have that:

$$w_1 \cdot S_1(Q, Q) \leq w_1 \cdot S_1(P, Q) \quad \forall P, Q \in \mathcal{P}(\mathcal{Y}),$$

and similar for S_2 . By adding the two inequalities, we have therefore that:

$$w_1 \cdot S_1(Q, Q) + w_2 \cdot S_2(Q, Q) \leq w_1 \cdot S_1(P, Q) + w_2 \cdot S_2(P, Q) \quad \forall P, Q \in \mathcal{P}(\mathcal{Y}),$$

which implies that S_+ is a proper SR.

Assume now additionally that S_1 , without loss of generality, is strictly proper, i.e.:

$$w_1 \cdot S_1(Q, Q) < w_1 \cdot S_1(P, Q) \quad \forall P, Q \in \mathcal{P}(\mathcal{Y});$$

then, summing the above with the corresponding inequality for S_2 gives that:

$$w_1 \cdot S_1(Q, Q) + w_2 \cdot S_2(Q, Q) < w_1 \cdot S_1(P, Q) + w_2 \cdot S_2(P, Q) \quad \forall P, Q \in \mathcal{P}(\mathcal{Y}),$$

which implies that S_+ is a strictly proper SR. \square

B. Stochastic Gradient Descent for generative-SR networks

B.1. Unbiased scoring rule estimates

Consider we have draws $\mathbf{x}_j \sim P, j = 1, \dots, m$.

Energy Score An unbiased estimate of the energy score can be obtained by unbiasedly estimating the expectations in $S_E^{(\beta)}(P, \mathbf{y})$ in Eq. (3.1):

$$\hat{S}_E^{(\beta)}(P, \mathbf{y}) = \frac{2}{m} \sum_{j=1}^m \|\mathbf{x}_j - \mathbf{y}\|_2^\beta - \frac{1}{m(m-1)} \sum_{\substack{j,k=1 \\ k \neq j}}^m \|\mathbf{x}_j - \mathbf{x}_k\|_2^\beta.$$

Kernel Score Similarly to the energy score, we obtain an unbiased estimate of $S_k(P, y)$ by:

$$\hat{S}_k(P, \mathbf{y}) = \frac{1}{m(m-1)} \sum_{\substack{j,k=1 \\ k \neq j}}^m k(\mathbf{x}_j, \mathbf{x}_k) - \frac{2}{m} \sum_{j=1}^m k(\mathbf{x}_j, \mathbf{y}).$$

Variogram Score It is immediate to obtain an unbiased estimate of $S_p(P, \mathbf{y})$ by:

$$\hat{S}_p(P, \mathbf{y}) = \frac{1}{m} \sum_{k=1}^m \sum_{i,j=1}^d w_{ij} (|y_i - y_j|^p - |x_{k,i} - x_{k,j}|^p)^2.$$

B.2. Unbiased estimate for $\nabla J(\phi)$

We now give more details on how to get unbiased gradient estimates for the training objective $J(\phi)$ in Eq. (4), in the case in which $S(P, \mathbf{y}) = \mathbb{E}_{\mathbf{Y}, \mathbf{Y}' \sim P} [g(\mathbf{Y}, \mathbf{Y}', \mathbf{y})]$ for some function g , which encompasses all the Scoring Rules above, as well as any weighted sum of those. The training objective in Eq. (4) is therefore:

$$J(\phi) = \frac{1}{N} \sum_{t=k}^{n-l} \mathbb{E}_{\mathbf{Y}, \mathbf{Y}' \sim P(\cdot | \mathbf{y}_{t-k+1:t})} [g(\mathbf{Y}, \mathbf{Y}', \mathbf{y}_{t+l})] = \frac{1}{N} \sum_{t=k}^{n-l} \mathbb{E}_{\mathbf{Z}, \mathbf{Z}' \sim Q} [g(T_\phi(\mathbf{Z}; \mathbf{y}_{t-k+1:t}), T_\phi(\mathbf{Z}'; \mathbf{y}_{t-k+1:t}), \mathbf{y}_{t+l})].$$

As mentioned in the main text, we cannot in general compute the expectation above. Additionally, Stochastic Gradient Descent usually consider a small batch of training samples, obtained by considering a random subset $\mathcal{T} \subseteq \{k, k+1, \dots, n-l-1, n-l\}$. Therefore, the following unbiased estimator of $J(\phi)$ can be obtained, with samples $\mathbf{z}_{t,j} \sim Q, j = 1, \dots, m$:

$$\hat{J}(\phi) = \frac{1}{|\mathcal{T}|} \sum_{t \in \mathcal{T}} \frac{1}{m(m-1)} \sum_{\substack{i,j=1 \\ i \neq j}}^m g(T_\phi(\mathbf{z}_{t,i}; \mathbf{y}_{t-k+1:t}), T_\phi(\mathbf{z}_{t,j}; \mathbf{y}_{t-k+1:t}), \mathbf{y}_{t+l}).$$

In practice, we then use autodifferentiation libraries (see for instance [Paszke et al., 2019](#)) to compute the gradient of the latter expression, which is an unbiased estimate of $\nabla J(\phi)$.

$$\begin{aligned} J(\phi) &= \frac{1}{N} \nabla_\phi \sum_{t=k}^{n-l} \mathbb{E}_{\mathbf{Z}, \mathbf{Z}' \sim Q} [g(T_\phi(\mathbf{Z}; \mathbf{y}_{t-k+1:t}), T_\phi(\mathbf{Z}'; \mathbf{y}_{t-k+1:t}), \mathbf{y}_{t+l})] \\ &= \frac{1}{N} \sum_{t=k}^{n-l} \mathbb{E}_{\mathbf{Z}, \mathbf{Z}' \sim Q} [\nabla_\phi g(T_\phi(\mathbf{Z}; \mathbf{y}_{t-k+1:t}), T_\phi(\mathbf{Z}'; \mathbf{y}_{t-k+1:t}), \mathbf{y}_{t+l})]. \end{aligned}$$

C. Performance measures for the probalistic forecast

C.1. Deterministic performance measures

We discuss two measures of performance of a deterministic forecast \hat{y}_{t+l} for a realization y_{t+l} ; across our work, we take \hat{y}_{t+l} to be the mean of the probability distribution $P_\phi(\cdot | \mathbf{y}_{t-k+1:t})$.

C.1.1. NORMALIZED RMSE

We first introduce the Root Mean-Square Error (RMSE) as:

$$\text{RMSE} = \sqrt{\frac{1}{N} \sum_{t=1}^N (\hat{y}_{t+l} - y_{t+l})^2},$$

where we consider here for simplicity $t = 1, \dots, N$. From the above, we obtain the Normalized RMSE (NRMSE) as:

$$\text{NRMSE} = \frac{\text{RMSE}}{\max_t \{y_{t+l}\} - \min_t \{y_{t+l}\}}.$$

NRMSE = 0 means that $\hat{y}_{t+l} = y_{t+l}$ for all t 's.

C.1.2. COEFFICIENT OF DETERMINATION

The coefficient of determination R^2 measures how much of the variance in $\{y_{t+l}\}_{t=1}^N$ is explained by $\{\hat{y}_{t+l}\}_{t=1}^N$. Specifically, it is given by:

$$R^2 = 1 - \frac{\sum_{t=1}^N (y_{t+l} - \hat{y}_{t+l})^2}{\sum_{t=1}^N (y_{t+l} - \bar{y})^2},$$

where $\bar{y} = \frac{1}{N} \sum_{t=1}^N y_{t+l}$. When $R^2 = 1$, $\hat{y}_{t+l} = y_{t+l}$ for all t 's.

C.2. Calibration error

We review here a measure of calibration of a probabilistic forecast; this measure considers the univariate marginals of the probabilistic forecast distribution $P_\phi(\cdot | \mathbf{y}_{t-k+1:t})$; for component i , let us denote that by $P_{\phi,i}(\cdot | \mathbf{y}_{t-k+1:t})$.

The calibration error ([Radev et al., 2020](#)) quantifies how well the credible intervals of the probabilistic forecast $P_{\phi,i}(\cdot | \mathbf{y}_{t-k+1:t})$ match the distribution of the verification $Y_{t+l,i}$. Specifically, let $\alpha^*(i)$ be the proportion of times the

verification $y_{t+l,i}$ falls into an α -credible interval of $P_{\phi,i}(\cdot|\mathbf{y}_{t-k+1:t})$, computed over all values of t . If the marginal forecast distribution is perfectly calibrated for component i , $\alpha^*(i) = \alpha$ for all values of $\alpha \in (0, 1)$.

We define therefore the calibration error as the median of $|\alpha^*(i) - \alpha|$ over 100 equally spaced values of $\alpha \in (0, 1)$. Therefore, the calibration error is a value between 0 and 1, where 0 denotes perfect calibration.

In practice, the credible intervals of the predictive are estimated using a set of samples from $P_{\phi}(\cdot|\mathbf{y}_{t-k+1:t})$.

D. General Lorenz96 model

The more general version of the Lorenz96 model presented in Section 6.2 is given by the following equations:

$$\begin{aligned}\frac{dx_k}{dt} &= -x_{k-1}(x_{k-2} - x_{k+1}) - x_k + F - \frac{hc}{b} \sum_{j=J(k-1)+1}^{kJ} y_j; \\ \frac{dy_j}{dt} &= -cb y_{j+1}(y_{j+2} - y_{j-1}) - c y_j + \frac{hc}{b} X_{\text{int}[(j-1)/J]+1}.\end{aligned}$$

The equations in Section 6.2 are recovered by setting $h = 1$, $b = 10$, $c = 10$ and $F = 20$.

E. Additional experimental details

E.1. Tuning γ in the Gaussian kernel

Similar to what was suggested for instance in [Park et al., 2016](#) and [Pacchiardi & Dutta, 2021](#), we set γ in the Gaussian kernel in Eq. (3.1) to be the median of the pairwise distances $\|\mathbf{y}_i - \mathbf{y}_j\|$ over all pairs of observations $\mathbf{y}_i, \mathbf{y}_j, i \neq j$ in the validation window.

E.2. Lorenz63 model

The generative network is a Fully Connected NN with 5 hidden layers which takes as input the concatenation of the values in the observation window and a latent variable Z with size 1, and outputs a forecast for the next timestep.

In the GAN setting, the discriminator is a fully connected NN again, which takes as input the concatenation of the values in the observation window and the observation/forecast, and outputs a value between 0 and 1 indicating how confident the discriminator believes that is a fake sample.

E.3. Lorenz96 model

The generative network is a fully connected NN with 5 hidden layers which takes as input the concatenation of the observed values in the observation window (flattened to an $8 \cdot 10 = 80$ dimensional vector) and a latent variable \mathbf{Z} with size 8, thus producing a forecast for the next timestep.

Again, a fully connected NN is used for the discriminator in the GAN setup; it takes as input the flattened values of the observation window and the observation/forecast, and outputs a value between 0 and 1 indicating how confident the discriminator believes that is a fake sample.

For the Variogram score, we consider a weight matrix inversely proportional to the distance on the loop in which the x variables are connected:

$$w_{ij} = 1 / \min\{|i - j|, |j + 8 - i|\}$$

E.4. WeatherBench dataset

For the variogram score, we use a weight matrix which is inversely proportional to the Euclidean distance on the grid, by considering the longitudinal direction as a cycle. Specifically, by denoting the longitude and latitude of component i of \mathbf{y} as $\text{lon}_i, \text{lat}_i$, the weight matrix is defined as:

$$w_{ij} = (|\text{lat}_i - \text{lat}_j|^2 + \min\{|\text{lon}_i - \text{lon}_j|, |\text{lon}_j + 64 - \text{lon}_i|\}^2)^{-1/2},$$

where 64 is the number of longitude points on the grid.

F. Additional experimental results

F.1. Lorenz63 model

Figure 5 reports similar plots to what shown in Section 6.1 for the Kernel Score (Figure 2). Calibration is slightly worse than with the Energy Score, but still better than with GAN

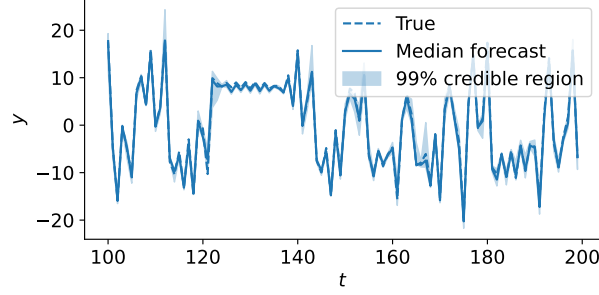


Figure 5. Results with the Kernel Score for the Lorenz63 model. The figure shows observations, median forecast and 99% credible interval for a portion of the test set.

F.2. Lorenz96 model

Figure 6 reports similar plots to what shown in Section 6.2 for the Kernel, Energy-Variogram and Kernel-Variogram Score (Figure 3).

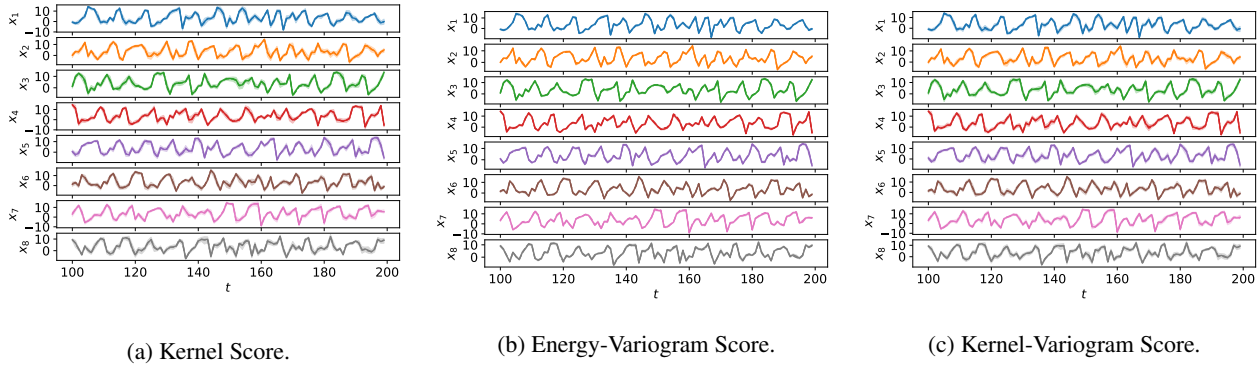


Figure 6. Results with the the Kernel, Energy-Variogram and Kernel-Variogram Scores for the Lorenz96 model. Panels show observations (dashed line), median forecast (solid line) and 99% credible interval (shaded region) for a portion of the test set. That is done for all 8 components of \mathbf{x} .

F.3. WeatherBench dataset

F.3.1. MAPS FOR A CHOSEN DATE

In Figure 7, we report realization and 5 different forecasts obtained with the Energy and Kernel Scores, in the same way as what was done for the Kernel-Variogram Score in Section 6.3 (Figure 4). In Figure 8, we report instead the differences between the realization and the 5 forecasts for all considered methods.

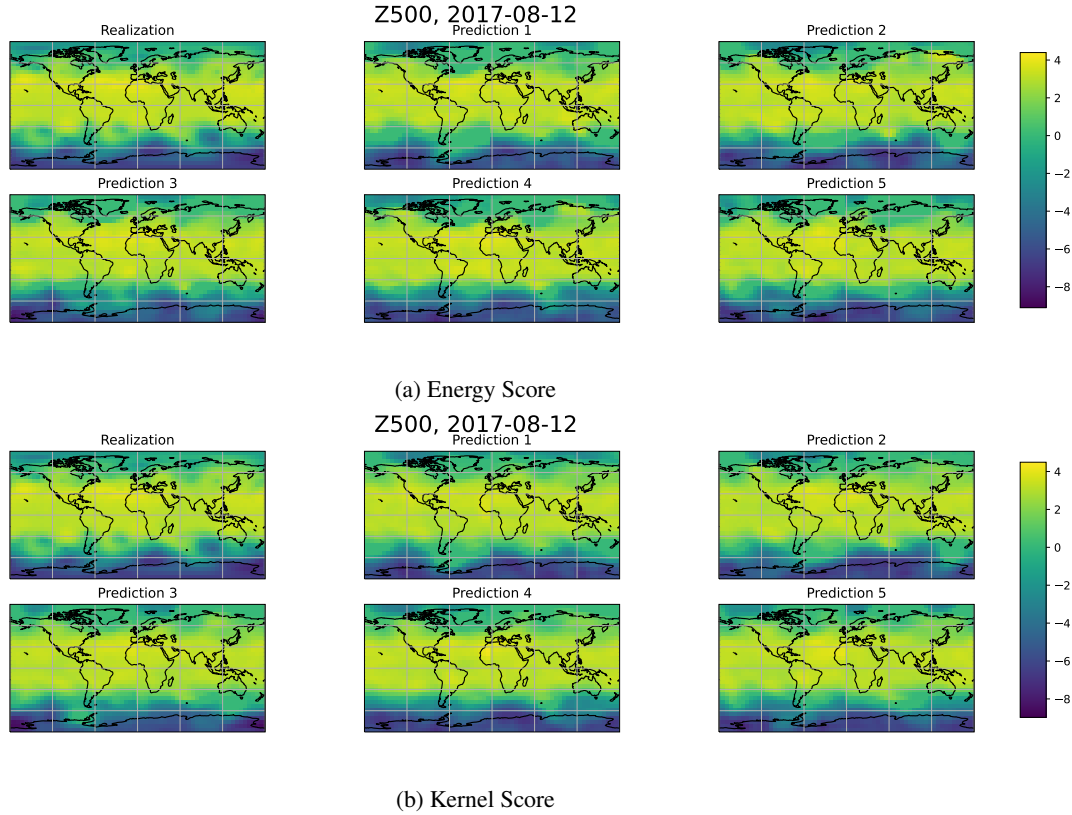


Figure 7. Realization and example of predictions obtained with the Energy and Kernel Scores for a specific date in the test set for the WeatherBench dataset. The predictions capture the main features but are slightly different one from the other.

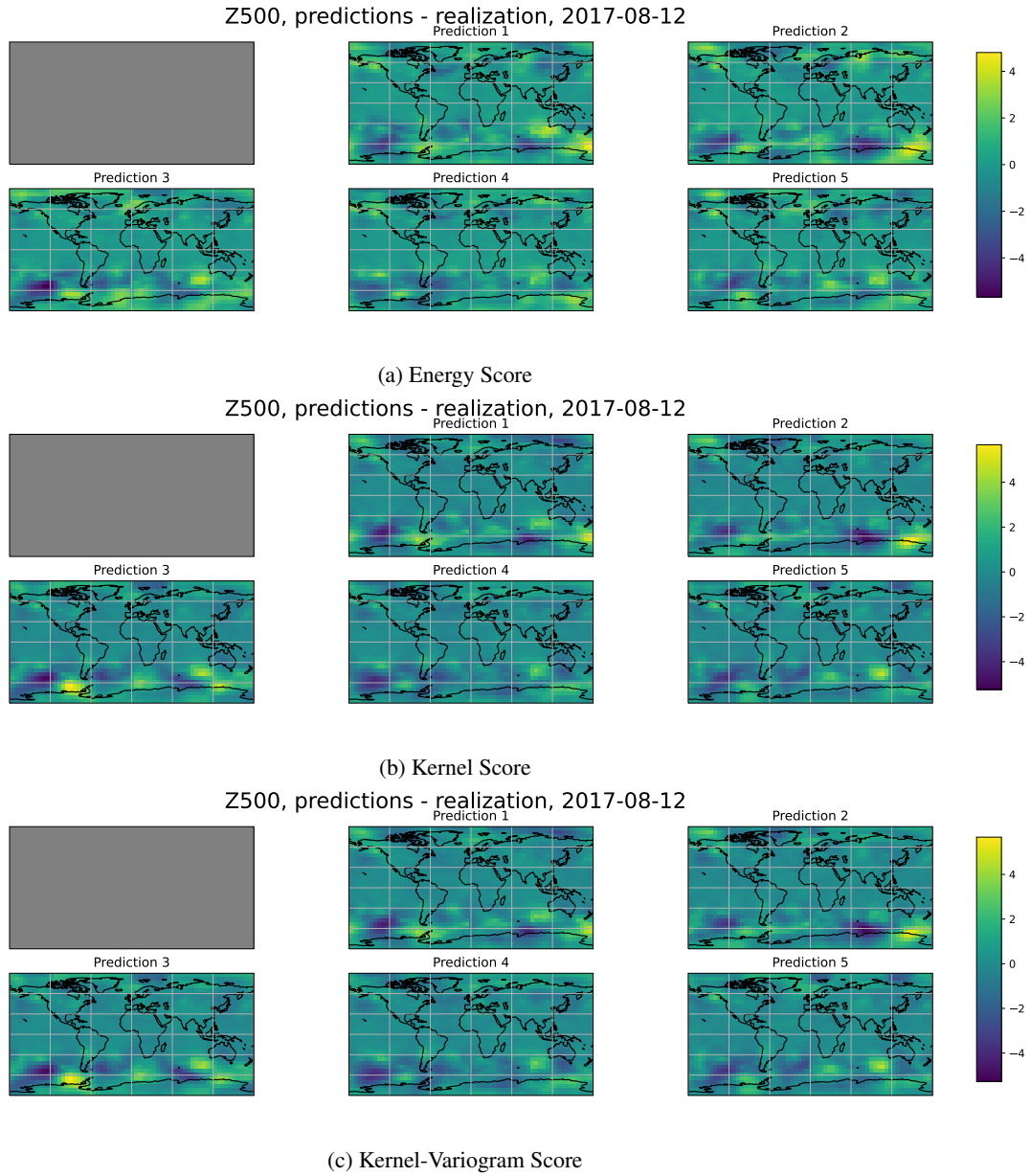


Figure 8. Difference between realization and prediction examples for the considered methods, for a specific date in the test set for the WeatherBench dataset.

F.3.2. TIME-SERIES PLOTS FOR SELECTED VARIABLES ON THE GRID

In Figure 9, we select 8 locations on the WeatherBench grid, and show the time series evolution, for a portion of the test period, for all considered methods.

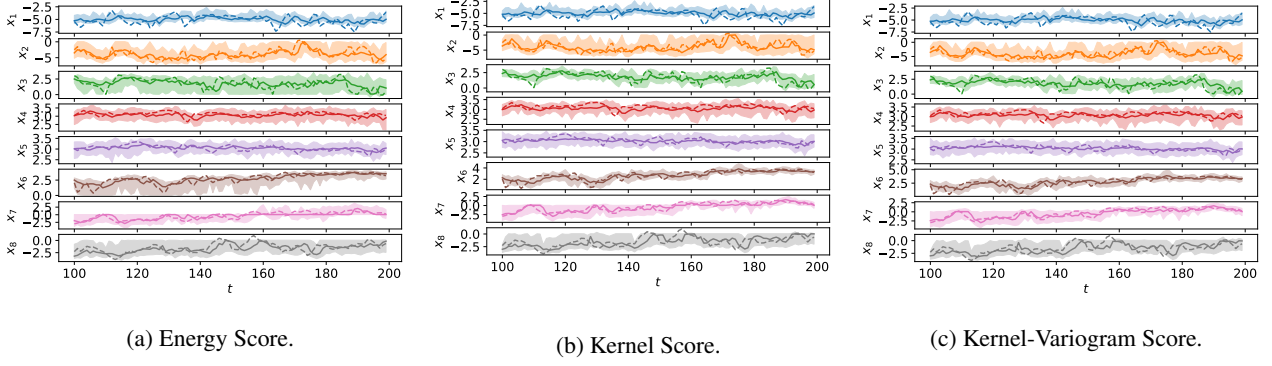


Figure 9. Results with the the Energy, Kernel and Kernel-Variogram Scores for 8 locations on the WeatherBench grid. The panels show observations (dashed line), median forecast (solid line) and 99% credible interval (shaded region) for a portion of the test set. That is done for all 8 components of \mathbf{x} .